ELSEVIER

Carbohydrate Research 315 (1999) 330–333

CARBOHYDRATE RESEARCH

Note

Imaging an alginate polymer gel matrix using atomic force microscopy

Alan W. Decho *

Department of Environmental Health Sciences, School of Public Health, University of South Carolina, Columbia, SC 29208, USA

Received 16 September 1998; accepted 6 December 1998

Abstract

The polysaccharide structure of alginic acid was examined as individual molecules and as dense gels using tapping-mode atomic force microscopy (AFM). Dilute (picomolar) non-ionic solutions of polymer molecules were sorbed onto mica surfaces. Under these conditions, the molecules exhibited frequent 'kinks' or abrupt right-angle changes in orientation. It is proposed that the kinks may correspond to chair backbone configurations that are predicted from the molecular structure of alginate, and occur at linkages between the monomers: α-L-guluronate (G) and β-D-mannuronate (M). Dense alginate gels (2% concentration) generated under strong ionic conditions (30 parts per thousand seawater) assumed a repeatable steric arrangement, and exhibited a relative regular spacing of solvent cavities (namely, H_2O) within the gel. This suggests that cation bridges are formed at regular intervals along adjacent polymers under these conditions. This work demonstrates the utility of tapping-mode AFM for examining the structure and gel conformation of a pliant polymeric matrix.

Keywords: Extracellular polymers; Alginate; Polysaccharide; AFM; Structure

Extracellular polysaccharides (EPS) produced by bacteria, microalgae, and macroalgae are molecules of applied and environmental importance. EPS form the anchoring mechanism for biofilm formation [1], and contribute to microbial-induced metal corrosion, dental plaque formation, and a variety of human disease processes [2].

The physical properties of EPS are largely determined by interactions of their chemical structure with the surrounding ionic environment. The large molecular weight (generally >100 kDa) and anionic nature of EPS allow these molecules to exist in a continuum of physical states, ranging from dense gels to dilute solutions. Imaging and quantifying the interactions between adjacent molecules of EPS are important to understanding how physical transitions occur between gel and solution states, and more generally, in mediating biofilm formation.

Atomic force microscopy (AFM) [3] is a potential tool for observing individual polymer molecules, and further, how they interact in forming a gel matrix. We imaged alginate molecules in both gel and solution states using AFM. Alginate used in this study is derived from the seaweed *Macrocystis pyrifera*. Alginate is a heteropolymer, generally greater than 130 kDa in size, and is composed of two acidic monomers: (1→4)-linked α-L-guluron-

* Fax: +1-803-777-3391.
E-mail address: adecho@sph.sc.edu (A.W. Decho)

0008-6215/99/$ - see front matter
PII: S0008-6215(99)00006-3

ate (G) and (1→4)-linked β-D-mannuronate (M). The residues are arranged in irregular blocks along a linear chain [4]. The gel properties of alginate are largely due to cation bridges between adjacent molecules. Therefore, additions of divalent cations, (mainly Ca^{2+} and Mg^{2+} ions) will facilitate gel formation. The binding of Ca^{2+} by algal alginate has been shown to be almost entirely due to the chelation of the cation by G-block regions of the polymer [5–7]. We used these properties to manipulate gel and solution states of alginate in order to observe the structure of single molecules and polymer networks (that is, gels).

All images were collected with a BioScope (Digital Instruments, Santa Barbara, CA) atomic force microscope on an Axiovert 135 (Carl Zeiss, Thornwood, NY) inverted microscope using a NanoScope III controller and computer (Digital Instruments). Vibration isolation was attained through the use of an invar stainless steel stage securely fastened to the optical microscope for high-frequency stability and a silicon gel cushion under the microscope for low-frequency stability. The intermittent contact or 'tapping' mode [8] was used to image samples. Height images recorded in the light tapping mode accurately reproduce the true topography of soft samples [9]. The scan range for a specimen in the tapping mode was typically less than 2 μm. For observation of hydrated specimens, a triangular 200 μm long, 20 μm wide cantilever with a pyramidal tip was mounted in a BioScope fluid cell holder. Therefore, specimens could be observed under seawater conditions. Optical data were captured with an integrating charge-coupling device (CCD) camera stored in digital format using NIH Image software (Version 1.55) and a frame-grabber board (Data Translation, Marlboro, MA). Adobe Photoshop 5.0 (Adobe Systems, San Jose, CA) was utilized for subsequent image processing.

In order to observe individual molecules using AFM, we used very dilute suspensions (10^{-10} M, final concentration) of sodium alginate (Sigma, St. Louis, MO) dissolved in distilled H_2O. To deposit alginate molecules onto newly cleaved sheets of mica, a small volume (100 μL) of alginate suspension was pipetted briefly (~5 s) onto the mica surface, then quickly removed by pipette. The surface was air dried (1 h) in a dust-free enclosure, then imaged using AFM.

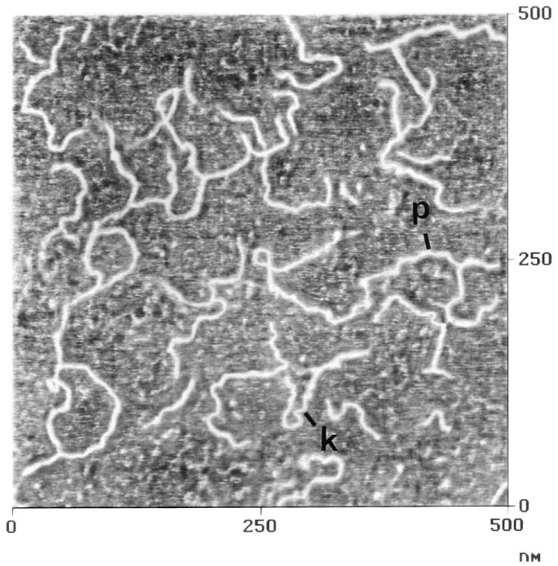

Fig. 1. An enlarged AFM image of alginate molecules (image size 500 × 500 nm) sorbed on a freshly prepared mica surface. Note abrupt angled changes or 'kinks' (k) in the molecular shape of polymers (p).

The structure of alginate has been well characterized ([10–13] and others). Fig. 1 shows a representative image obtained for alginate samples derived from dilute solutions. Areas of low polymeric coverage show individual alginate molecules and thicker strands (Fig. 1). Tracing across individual alginate strands provides an estimate of width of the macromolecule, by measuring the molecular height relative to the mica surface (Fig. 1). Our measurements show that the width of single strands (Fig. 2) varies

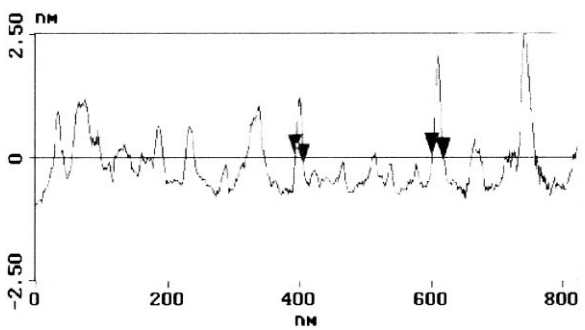

Fig. 2. Image analysis of a typical cross-section of single strands of alginic acid polymers on a mica surface. The thickness is determined by height (nm) on the y-axis (vertical). Arrows represent markers for width measurements (data not shown).

between 1.41 and 4.65 nm ($n = 20$). These measurements appear to overestimate the width when compared to those derived from X-ray diffraction studies of similar glucopyranosyl molecules. The polysaccharide, scleroglucan, which is a $(1 \rightarrow 6)$-branched $(1 \rightarrow 3)$-β-D-linked glucan, was shown to have a single-strand polymer width of 0.55 nm based on X-ray diffraction measurements [14]. Measurements using non-contact mode AFM have shown the width of scleroglucan to be 1 nm [15]. The observed differences between measurements derived from X-ray diffraction and AFM may occur because the chain thickness is convoluted with the thickness of the AFM measuring tip, a probe-broadening effect [16]. A second possibility is that the thicker strands may represent a side-by-side association of molecules.

The observed variability in the widths of alginate molecules may be explained, in part, by the physical structure of the molecule. The two monomers G and M occur in three major types of blocks [17]. In their most favored chair conformations, $^4C_1$ and $^1C_4$, respectively, monomers are arranged as a series of block structures consisting of M-blocks (–M–M–M–M–); G-blocks (–G–G–G–G–) and M–G-blocks (–M–G–M–G–). When an M–G block is present, there will be an abrupt right-angle change in the orientation of the polymer molecule [17]. It is suggested here that the 'kinks', when observed in single molecule preparations as in Fig. 1, correspond to –M–G– or –G–M– linkages. Loops or possible bifurcations were also observed. A bifurcation may represent a region where there is an unraveling of adjacent helices into individual strands.

To prepare alginate gels, we used artificial seawater containing abundant Ca^{2+} and Mg^{2+} ions. It was prepared according to the Marine Biological Laboratory (MBL) Formula for Trace Sea Water, using NaCl = 24.73; KCl = 0.62; $CaCl_2 \cdot 2H_2O = 1.36$; $MgCl_2 \cdot 6H_2O = 4.66$; $MgSO_4 \cdot 7H_2O = 6.29$; KBr = 0.089; NaF = 0.003; $SrCl_2 \cdot 6H_2O = 0.037$; $H_3BO_3 = 0.024$ g/L dissolved in ultraclean water (18.2 MΩ), adjusted to 30 parts per thousand salinity, and held at a constant pH (8.0) and temperature (23 °C). A 2% alginate solution was made by dissolving sodium alginate (Sigma) in deionized water (dH_2O). Because the matrices of thick gels (greater than 40–50 μm thickness) on a mica surface tend to exhibit nonspecific vibrations even when isolated on vibration-reducing tables, they could not be used. Instead, we prepared very thin gels by smearing the concentrated alginate solution over a clean mica surface, then adding 1 mL of artificial seawater. The addition of cations, mainly Ca^{2+} and Mg^{2+}, present in the seawater rapidly transformed the smeared alginate solution into a thin gel on the surface of the mica. This reduced nonspecific vibration and greatly enhanced the resolution of images.

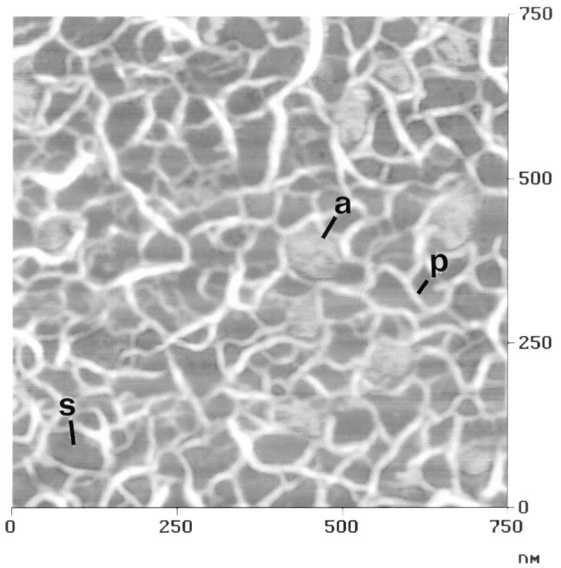

Fig. 3. An enlarged AFM image of an alginate gel (2%) in seawater (30 ppt salinity). (s, solvent cavity; p, polymer; a, artifact).

The gel structure, when observed using AFM, exhibited a repeating network of solvent cavities and polymeric strands (Fig. 3). The diameter of solvent cavities ranged between 22 and 58 nm. The measured thickness of polymer strands in the gel matrix ranged from 3.74 to 18.2 nm. Since the thickness of the gel-strands was greater than those estimated for individual polymeric molecules (1–3 nm), this suggests that the gel-strands may represent several polymer molecules arranged as an aggregate. Such an arrangement would potentially contribute to a physically stronger

gel matrix. Artifacts were observed in AFM images of gel matrices (Fig. 3). These were likely to be due to lateral or shear forces exerted by the tip which cause surface features to be swept aside or smeared out [18].

Another study [16] has utilized immersion in butanol or other alcohols for imaging polymeric molecules using the contact mode. This improves overall resolution, when compared with immersion in water. However, alcohols were not used in our study since they precipitate polysaccharides and would alter the gel structure.

The present study demonstrates the utility of tapping-mode AFM for observing individual chains and gel network structure of alginate. Estimations of molecular size, however, must be viewed conservatively since resolution is close to the limit imposed by experimental conditions.

Acknowledgements

The author acknowledges Sophia Hohlbauch (Digital Instruments) for her assistance in AFM work, and the kind support of the staff at Digital Instruments. All AFM imaging work was conducted at Digital Instruments, Santa Barbara, CA. This work was supported by grants from the National Science Foundation (OCE 96-17738) and the Office of Naval Research (NOOO14-97-10024). This represents RIBS contribution # 002.

References

[1] A.W. Decho, *Oceanogr. Mar. Biol. Ann. Rev.*, 28 (1990) 73–153.
[2] J.W. Costerton, Z. Lewandoski, D. DeBeer, D.E. Caldwell, D.R. Korber, G. James, *J. Bacteriol.*, 176 (1994) 2137–2142.
[3] H.G. Hansma, J.H. Hoh, *Ann. Rev. Biophys. Biomol. Struct.*, 23 (1994) 115–139.
[4] H. Grasdalen, B. Larsen, O. Smidsrød, *Carbohydr. Res.*, 89 (1981) 179–191.
[5] O. Smidsrød, A. Haug, *Acta. Chem. Scand.*, 26 (1972) 17–28.
[6] E.R. Morris, D.A. Rees, D. Thom, J. Boyd, *Carbohydr. Res.*, 60 (1978) 145–154.
[7] C.M. DeRamos, A.E. Irwin, J.L. Nauss, B.E. Stout, *Inorg. Chim. Acta*, 256 (1997) 69–75.
[8] Q. Zhong, D. Inniss, K. Kjoller, V.B. Elings, *Surf. Sci. Lett.*, 290 (1993) L688–L692.
[9] S. Magonov, Y. Godovsky, *Am. Lab.*, 30 (1998) 15–21.
[10] O. Smidsrød, *Faraday Discuss. Chem. Soc.*, 37 (1974) 263–274.
[11] H. Zhang, H. Zheng, Q. Zhang, J. Wang, M. Konno, *Biopolymers*, 46 (1998) 395–402.
[12] K.I. Draget, G.S. Braek, O. Smidsrød, *Carbohydr. Polym.*, 25 (1994) 31–38.
[13] B.T. Stokke, K.I. Draget, Y. Yuguchi, H. Urakawa, K. Kajiwara, *Macromol. Symp.*, 120 (1997) 91–101.
[14] T.L. Bluhm, Y. Deslandes, R.H. Marchessault, S. Perez, M. Rinaudo, *Carbohydr. Res.*, 100 (1982) 117–130.
[15] T.M. McIntire, D.A. Brant, in R.R. Townsend, A.T. Hotchkiss (Eds.), *Techniques in GlycoBiology*, Marcel Dekker, New York, 1997, pp. 187–208.
[16] A.R. Kirby, A.P. Gunning, V.J. Morris, *Carbohydr. Res.*, 267 (1995) 161–166.
[17] C.E. Chitnis, D.E. Ohman, *J. Bacteriol.*, 172 (1990) 2894–2900.
[18] C.A.J. Putman, K.O. van der Werf, B.G. de Grooth, N.F. van Hulst, J. Greve, *Biophys. J.*, 67 (1994) 1749–1753.